JOURNAL OF THERMOPHYSICS AND HEAT TRANSFER
Vol. 17, No. 3, July–September 2003

Recovery Temperature Measurement of Underexpanded Sonic Jets Impinging on a Flat Plate

Byung Gi Kim,* Man Sun Yu,* and Hyung Hee Cho†
Yonsei University, Seoul 120-749, Republic of Korea

An experimental investigation has been carried out to examine heat-transfer characteristics of an axisymmetric, underexpanded, sonic jet impinging on a flat plate. The ratio of nozzle-exit pressure to the ambient pressure, that is, underexpansion ratio ranges from 1.5 to 3.5, and the distance from the nozzle exit to the plate is adjusted from 0.5 to 20.0 nozzle-exit diameters. Detailed measurements of the recovery factor and the surface pressure on the flat plate have been achieved. The results showed that the recovery factor obtained in the present study have distributions that are different from those for low-velocity jets. It has been found that the recovery factor at the stagnation point varies from 0.35 up to over 1.25 for the highest underexpansion ratio of $P_e/P_a = 3.5$ within the present experimental range.

Nomenclature

C_p	=	specific heat of air
D_{NE}	=	nozzle-exit diameter
Ma	=	Mach number
M_D	=	design Mach number at the nozzle exit
P_a	=	ambient pressure
P_c	=	pressure in the settling chamber
P_e	=	pressure at the nozzle-exit plane
R	=	radial distance from the center
r	=	recovery factor
T_{aw}	=	adiabatic wall temperature
T_d	=	dynamic temperature of a jet
T_s	=	static temperature of a jet
T_0	=	total temperature of a jet
u_j	=	velocity of a jet at the nozzle exit
Z	=	axial distance from the nozzle-exit plane
Z_{MR}	=	distance from the nozzle to reflection position for Mach reflection
Z_P	=	nozzle-to-plate distance
Z_{RR}	=	distance from the nozzle to reflection position for regular reflection
γ	=	specific heat ratio
Δ_1	=	length of the first shock cell

I. Introduction

WHEN high-pressure gas expands through a nozzle into atmosphere, the flow state of a jet is varied depending upon the pressure ratio through the nozzle. An underexpanded jet is obtained if the pressure at the nozzle exit is greater than the ambient pressure. When a flat plate is inserted into the near field of the underexpanded freejet, the flow structure is significantly disturbed. Figure 1 shows the shock structure in the near field of the underexpanded impinging jet. A stand-off shock occurs ahead of the plate, and the flow decelerates through the shock. Owing to the interaction of the stand-off shock with the intercepting shock in a freejet, the reflected shock is formed. The subsonic region behind the stand-off shock is separated from the supersonic flow behind the oblique reflected shock by the slip surface, and mixing zone is developed along the slip surface. As the shock-layer fluid moves radially outward, the flow reaccelerates, and the wall jet region starts to be developed. A shear layer grows along the constant-pressure upper boundary of this wall jet and a boundary layer along the surface of the plate. The wall-jet velocity is reduced by gradual growth and merging of these viscous layers.

Various situations associated with the impingement of an underexpanded jet onto a solid object can be found in engineering applications. Among them, launch of a rocket, the takeoff and landing of V/STOL aircraft, impingement of a jet-engine exhaust, and the thrust vector control system of a solid rocket motor are some examples given frequently. Because dynamic energy is converted to thermal energy, impingement of high-temperature flow like exhaust flumes can produce severe thermal loads as well as aerodynamic loads on the target surface. As results of extensive studies conducted by many researchers, some of the interesting and complex phenomena have been revealed to us, but not satisfactorily yet. A large portion related to this subject still remains unknown. A number of previous investigations associated with the underexpanded impinging jets have concentrated mainly on the basic aspects of flow structure: complex shock structures and interactions have been extensively studied using optical methods such as a shadowgraph and a schlieren method,[1–6] and comparisons with the theoretical predictions also have been made.[3,7,8] Measurement of pressure distributions on the target surface has revealed an intriguing phenomenon of stagnation bubble, which occurs around the stagnation point.[1–5,7,9] Since the 1990s, there have been several attempts to simulate numerically the flowfield of supersonic impinging jet.[6,10–12] In contrast to numerous investigations related to flow structures, very few data are available for heat-transfer characteristics of the underexpanded impinging jets at present.[13] Fox et al.[14] introduced a conceptual model for the separation of total temperature by vortical structure to explain the experimental data taken at high subsonic Mach numbers, and in their extended study on energy separation, Fox and Kurosaka[15] showed that the unsteady movement of shock structure disrupted by the formation and movement of vortices causes total temperature separation for underexpanded jets. Although they mentioned the shock-induced cooling on the impinging plate, they presented the results only for the total temperature distributions in the freejets.

The objective of the present study is to obtain basic heat-transfer information on an underexpanded sonic jet, which impinges on a flat plate. An experimental investigation has been carried out to examine heat-transfer characteristics of an axisymmetric underexpanded sonic jet. Distributions of recovery factor on the flat plate have been obtained in detail. In addition, distributions of surface pressure on the flat plate have been measured, and the shock structures in the underexpanded jets have been visualized employing a shadowgraph method. As the parameters of interest, the followings have been considered: one is the underexpansion ratio, which is defined by

Received 21 October 2002; revision received 13 February 2003; accepted for publication 17 February 2003.

*Graduate Student, Department of Mechanical Engineering.
†Professor, Department of Mechanical Engineering, 134, Shinchong-dong, Seodaemun-gu; hhcho@yonsei.ac.kr. Member AIAA.

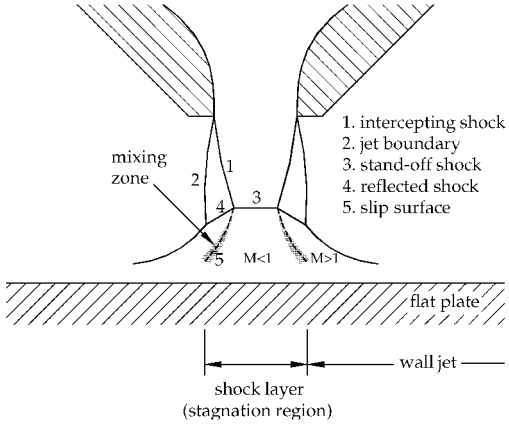

Fig. 1 Schematic diagram of an underexpanded impinging jet.

the ratio of the nozzle-exit pressure to the ambient pressure. Both moderately underexpanded cases and highly underexpanded cases are included. The other is the nozzle-to-plate distance. The emphasis is on the small nozzle-to-plate distances within the first shock cell. However, the results in the far field also have been obtained. The results of the present study would provide basic information to understand unknown aspects of heat transfer associated with underexpanded sonic jet impinging on a flat plate, and they might be used to verify the future numerical model related to sonic impinging jets.

II. Experimental Apparatus

Figure 2 shows the schematic diagram of experimental apparatus used for the present investigation. Air is compressed up to 150 kgf/cm^2 by reciprocating compressors and passes through seven stage air filters to remove moisture and oil. Then, it is stored in six storage tanks. Total storage capacity of tanks is 0.69 m^3. The compressed air is supplied to the settling chamber through regulators (Yamato sangyo, YR-5062) from the storage tanks. The nozzle, from which a jet issues, is mounted on the settling chamber. A contoured convergent nozzle is used in the present experiments. The nozzle has the exit diameter of 10.0 mm and a design Mach number of 1.0. After stagnating at the settling chamber, the air is accelerated in the nozzle and then injected into the atmosphere. Settling chamber is a cylinder made of stainless steel, of which the length and the diameter are 330 and 150 mm, respectively. The pressure under stagnation condition is measured using a pressure transducer (Pureron, PC-302A-VR), which is mounted on the chamber wall, and the temperature is measured by a T-type thermocouple. The pressure in the settling chamber is carefully controlled by pressure regulators. The nozzle pressure ratio is maintained constant during a run within ±1% of the designated value. Owing to the pressure drop in the storage tanks and through the regulators during a run, the temperature of supplied air decreases continuously. To keep the total temperature of a jet constant and to minimize the temperature difference with the ambient air, the supplied air is heated with an electric heater. The electric power input to the heater is controlled automatically during a run by comparing the readings of thermocouples, which measure the total temperatures at the settling chamber and the ambient temperature. Total temperature of a jet is adjusted close to the ambient air temperature within the difference of ±0.2°C.

The test plate consists of thermocouples and the backing of insulated layers. It is mounted on a two-dimensional positioning traverse to adjust the nozzle-to-plate distance precisely. The backside of the plate is insulated thermally with the air gap, the fiberglass, and the acrylic. The plate is instrumented with a row of 41 36-gauge T-type (copper-constantan) thermocouple junctions. They are spaced 2.5 mm apart within 60 mm across the span in the central portion, where significant variation of temperature is expected, and 5 mm apart outside the center region. Another plate with two pressure taps in the central portion is used for measurement of the surface pressure. The hole size is 0.8 mm in diameter, and the two pressure taps are spaced 20.0 mm. The pressure is measured by Druck pressure transducer (PMP4070) connected to each pressure tap. After the pressure taps are moved to the target position using the two-dimensional positioning traverse, the voltage signals from pressure transducers are scanned three times and averaged. The output signals from thermocouples and pressure transducers are scanned and acquired using data-acquisition/switch units (Agilent 34970A) equipped with three 16-channel multiplexer modules (HP 34902A) and stored in a personal computer. A shadowgraph method is used to visualize the shock structure in the flowfield of the jet.

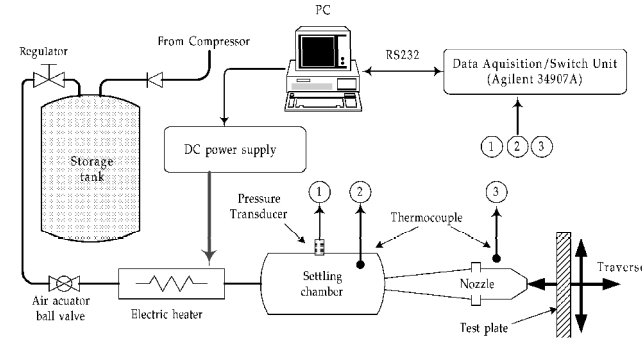

a)

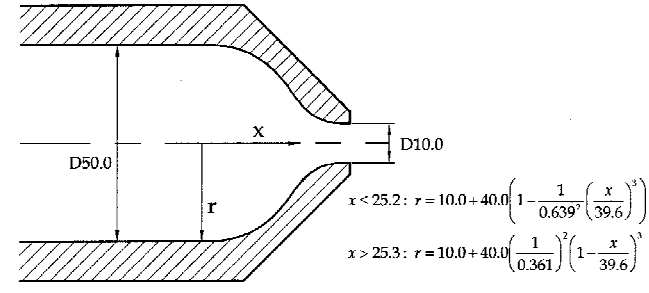

b)

Fig. 2 Schematic diagrams: a) experimental apparatus: 1, for stagnation pressure; 2, for total temperature; and 3, for ambient temperature; and b) nozzle geometry.

III. Data Reduction

The adiabatic wall temperature measurements are expressed in a dimensionless form using a recovery factor. It is defined by

$$r = (T_{aw} - T_s)/T_d = 1 + (T_{aw} - T_0)/T_d \tag{1}$$

The dynamic temperature of the jet in the preceding equation is calculated from the following relation:

$$T_d = \frac{u_j^2}{2C_P} = \frac{[(\gamma - 1)/2]M_D^2}{1 + [(\gamma - 1)/2]M_D^2} T_0 \tag{2}$$

The experimental uncertainties in recovery factor and pressure are calculated using the method of Kline and McClintock.[16] The uncertainties of the recovery factor and the pressure normalized with respect to the stagnation pressure measured in the settling chamber are within ±3.5 and ±2.1%, respectively, with a confidence level of 95%.

IV. Experimental Conditions

The underexpansion ratio is defined as the ratio of the nozzle-exit pressure to the ambient pressure P_e/P_a. The underexpansion ratio is tested from 1.5 to 3.5 for the sonic nozzle, and it corresponds to the nozzle pressure ratio (P_0/P_a) from 2.84 to 6.63. The nozzle pressure ratio is determined from the following relation:

$$P_0/P_a = (P_e/P_a)\left\{1 + [(\gamma - 1)/2]M_D^2\right\}^{\gamma/(\gamma - 1)} \tag{3}$$

Table 1 Shock structures of a freejet for various pressure ratios

Exit Mach number M_D	Underexpansion ratio P_e/P_a	Nozzle pressure ratio P_0/P_a	Type of reflection	Location of reflection Z_{RR} or Z_{MR}	Length of the first shock cell Δ_1
1.0	1.5	2.84	Regular	$0.6D_{NE}$	$1.0D_{NE}$
	2.0	3.79	Mach	$1.0D_{NE}$	$1.4D_{NE}$
	2.5	4.73	Mach	$1.2D_{NE}$	$1.6D_{NE}$
	3.5	6.63	Mach	$1.5D_{NE}$	$2.0D_{NE}$

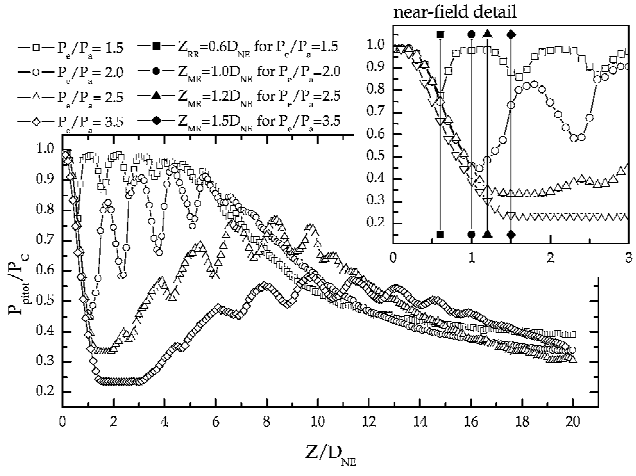

Fig. 3 Distributions of pitot pressure along the centerline for a freejet: |, positions of shock reflection obtained from the shadowgraphs.

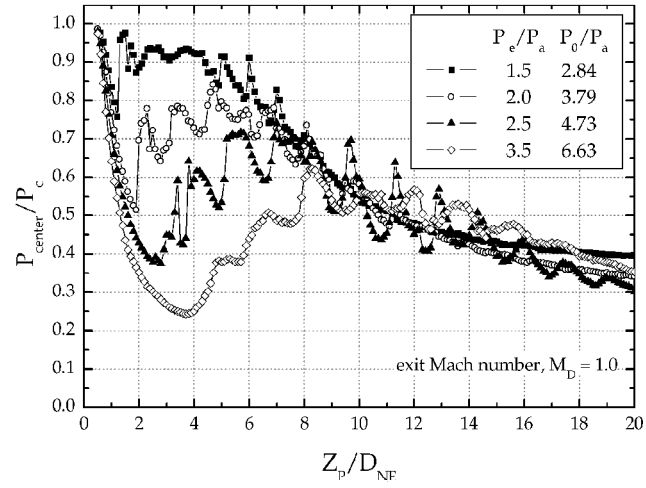

Fig. 4 Variation of the central surface pressure for an impinging jet.

The nozzle-to-plate distance is changed in the range from a half nozzle-exit diameter to 20 diameters. The detailed measurements have been conducted mainly at the small nozzle-to-plate distances.

V. Results and Discussion

A. Freejets

It is readily expected that characteristics of an underexpanded impinging jet are closely related to periodic variation of flow structures in a freejet as a result of the existence of the shock cell structure in it. Before proceeding to our main concerns of the underexpanded sonic impinging jets, some basic information on the underexpanded freejets for the sonic nozzle has been obtained.

Figure 3 presents the variation of the pitot pressure along the centerline of the freejets. The pitot pressure is normalized with respect to the stagnation pressure measured at the settling chamber P_c. The distance from the nozzle exit is denoted by Z, and it is also normalized with respect to the nozzle exit diameter D_{NE}. The pitot pressure decreases initially as the distance from the nozzle exit is increased because the flow expands and accelerates downstream of the nozzle exit. Note that the flow downstream of the nozzle exit accelerates over $Ma = 1$. When a pitot probe is placed in the supersonic flow, a shock wave forms ahead of the nose of the probe, and the total pressure decreases across the shock. Such expansion continues until the tip of the pitot probe is moved behind the position where the intercepting shock reflects at the centerline for $P_e/P_a = 1.5$ or Mach disk occurs for $P_e/P_a = 2.0$, 2.5, and 3.5. The expansion and compression continues to occur periodically in the downstream direction until the flow becomes subsonic by the turbulent mixing and viscous effect is dominant over the whole field. The location of Mach disk and the length of the first shock cell obtained from the shadowgraphs are summarized in Table 1.

B. Impinging Jets

Distributions of Surface Pressure

Figure 4 presents the variation of the surface pressure at the center of the plate with the nozzle-to-plate distance. The central surface pressure decreases initially with increasing nozzle-to-plate distance, and subsequent rise and fall repeat in the downstream direction. For the sake of convenience, the nozzle-to-plate distance to which the central surface decreases initially is referred to as initial expansion length. Downstream of the initial expansion length, the central surface pressure rises steeply for the moderately underexpanded cases of $P_e/P_a = 1.5$ and 2.0. However, the behaviors downstream of the initial expansion length for the highly underexpanded cases are noticeably different from those for the moderately underexpanded cases. For $P_e/P_a = 2.5$, irregular rise and fall follow until the plate is moved to $Z_P/D_{NE} \cong 4.0$. On the other hand, the pressure rises smoothly to $Z_P/D_{NE} \cong 5.0$ for $P_e/P_a = 3.5$.

Figure 5 shows the change of shock structure for $P_e/P_a = 1.5$ when the plate is moved downstream of the initial expansion length. Abrupt rise in pressure for $P_e/P_a = 1.5$ occurs when the stand-off shock ahead of the plate is moved immediately downstream of Z_{RR}. Similar behavior is also shown in the case with $P_e/P_a = 2.0$. (Shadowgraph results are not presented here.) This can be explained as follows. As the plate is moved in downstream direction, the stand-off shock ahead of the plate also moves downstream with the plate. Total pressure loss across the shock increases because the upstream Mach number increases with increasing distance from the nozzle exit. Thus, central surface pressure within the initial expansion length decreases as the nozzle-to-plate distance increases. When the stand-off shock moves further downstream and recedes beyond Z_{RR}, the flow through the central shock diminishes and that through the oblique shock increases, as shown in Fig. 5c. This shock configuration is favorable to inward diffusion of outer flow with high total pressure, and consequently the pressure near the centerline steeply increases. However, for the highly underexpanded cases inward diffusion from outer region is less effective as a result of the existence of the subsonic region resulting from the large Mach disk, as shown in Fig. 6. Moreover, interaction of slip surface with the reflected shock makes the flow structure more complicated.

Figure 7 presents the radial profiles of the static pressure on the plate in the near field. The radial distance from the center of the plate is indicated by R, and it is normalized with respect to the nozzle exit diameter D_{NE}. Figure 7a shows surface-pressure profiles for $P_e/P_a = 1.5$. The thick vertical line in the graph represents the initial expansion length. When the plate is placed at

Table 2 Onset of maximum pressure off the center

Exit Mach number M_D	Underexpansion ratio P_e/P_a	Occurrence of peripheral pressure maximum		P_{max}/P_C
		Z_P/D_{NE}	R/D_{NE}	
1.0	1.5	1.1	0.4	0.84
	2.0	1.4	0.6	0.63
	2.5	1.8	0.8	0.49
	3.5	2.1	1.0	0.35

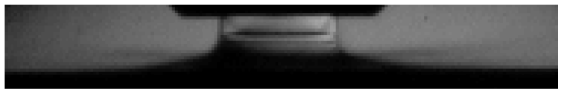

a) $Z_P/D_{NE} = 0.5$

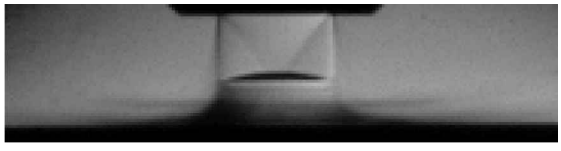

b) $Z_P/D_{NE} = 1.0$

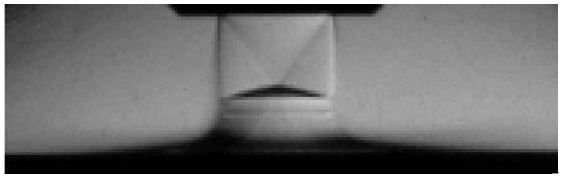

c) $Z_P/D_{NE} = 1.2$

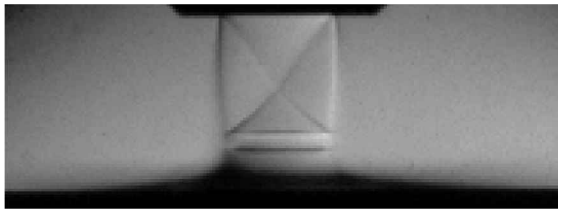

d) $Z_P/D_{NE} = 1.5$

Fig. 5 Shadowgraphs of impinging jets for $P_e/P_a = 1.5$.

$Z_P/D_{NE} = 0.5$, the surface-pressure profiles have a maximum at the center of the plate, and the pressure drops as the flow accelerates with increasing distance from the stagnation point. After slight recompression at $R/D_{NE} \cong 1.0$, the pressure approaches to the ambient pressure ($P_a/P_0 = 0.35$). As the plate is moved downstream to $Z_P/D_{NE} = 1.0$, the pressure in the shock layer decreases. It is because of increased total pressure loss across the central standoff shock with increasing upstream Mach number, as just mentioned. As the plate is moved further downstream, the maximum pressure occurs off the center. The surface pressure has a maximum at $R/D_{NE} \cong 0.4$ when the plate is placed at $Z_P/D_{NE} = 1.2$. Such a peripheral maximum of the pressure suggests that recirculating flow called a stagnation bubble occurs in the shock layer as reported previously by other researchers.[1,2,4] As the underexpansion ratio increases, the peripheral maximum occurs farther downstream, that is, at the larger nozzle-to-plate distance, and the radius of peripheral maximum also increases. The position and magnitude of peripheral maximum is summarized in Table 2. For the higher underexpansion ratios, as shown in Fig. 7b, the radial profiles of surface pressure have similar variations with increasing nozzle-to-plate distance, especially in the shock layer. However, the pressure distributions in the wall jet region are conspicuously changed at the small nozzle-to-plate distances with increasing underexpansion ratio. In the wall jet region, the surface pressure rises and falls periodically. The amplitudes of the periodic variation in pressure decay with radial distance, and the pressure becomes close to the atmospheric pressure gradually. This alternating compression and expansion region in the wall jet is produced by repeated reflections of the waves from the jet edge by the upper boundary of the wall jet and the plate surface.[3,7]

a) $Z_P/D_{NE} = 1.0$

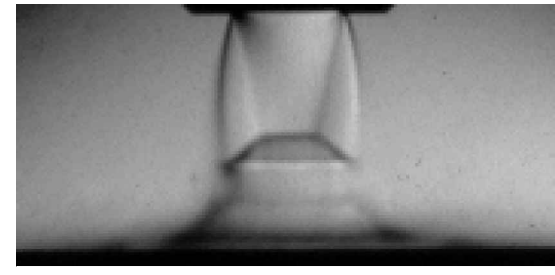

b) $Z_P/D_{NE} = 2.0$

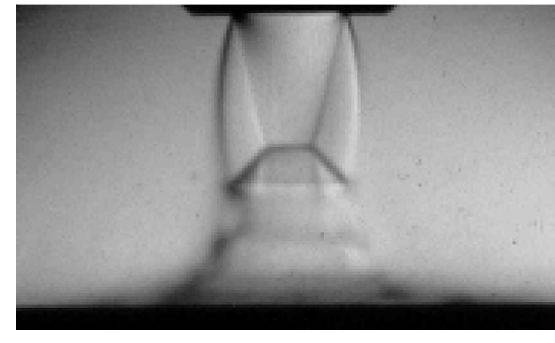

c) $Z_P/D_{NE} = 2.5$

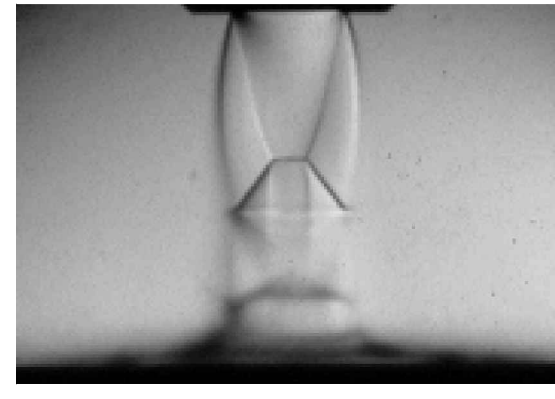

d) $Z_P/D_{NE} = 3.0$

Fig. 6 Shadowgraphs of impinging jets for $P_e/P_a = 2.5$.

In Fig. 7, it is also seen that pressure recovery occurs as the plate is moved downstream of the initial expansion length. It is because of increasing inward diffusion from the outer region behind the oblique shock. The pressure recovery occurs relatively steeply only for the moderately underexpanded cases because the central standoff shock diminishes significantly in size, as shown in Fig. 5.

Distributions of Recovery Factor

The measured adiabatic wall temperature is expressed in terms of recovery factor from Eq. (1). Figure 8 presents variation of the recovery factor at the stagnation point ($R/D_{NE} = 0$) with the nozzle-to-plate distance for various underexpansion ratios. The inserted graph presents the data at small nozzle-to-plate distances ($Z_P/D_{NE} \leq 3.0$) in detail. The recovery factor is slightly lower than

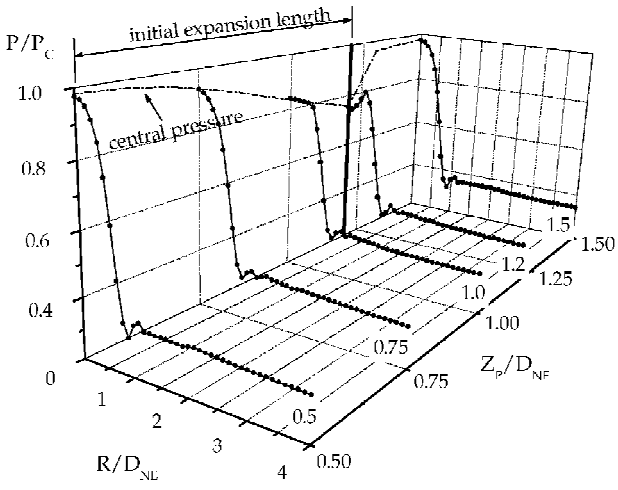

a) $P_e/P_a = 1.5$

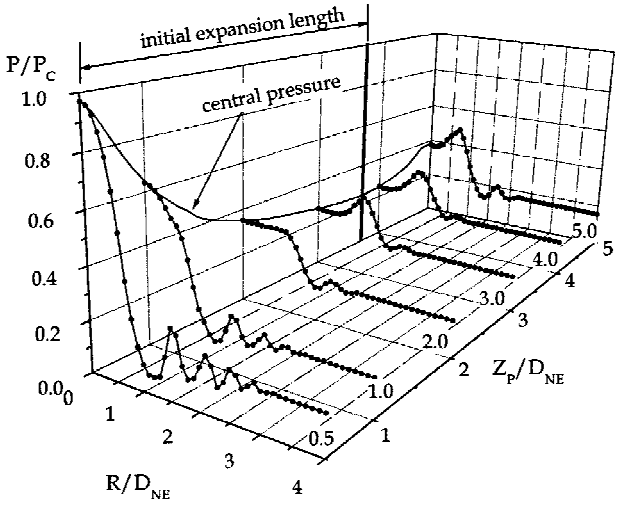

b) $P_e/P_a = 3.5$

Fig. 7 Radial distributions of the surface pressure in near field.

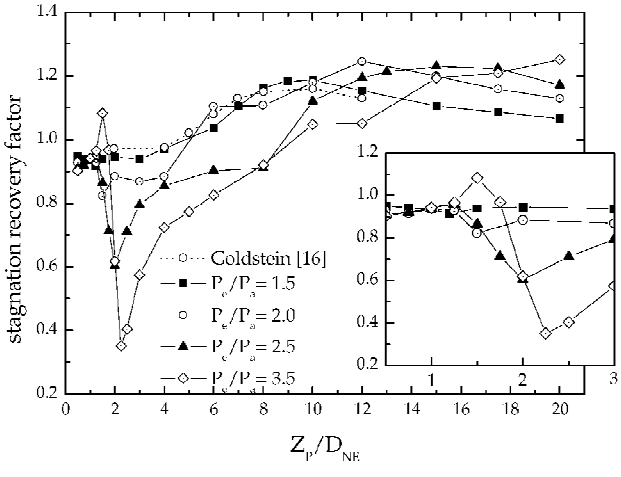

Fig. 8 Variation of the recovery factor at the stagnation point for various underexpansion ratios.

unity up to $Z_P/D_{\mathrm{NE}} \cong 1.0$ and then decreases steeply. This steep reduction in recovery factor implies that the temperature at the stagnation point is lower than the ambient temperature, that is, a cooling effect. The cooling increases in magnitude and persists farther downstream with increasing underexpansion ratio. The recovery factor for the subsonic impinging jet is replotted from Goldstein et al.[17] for comparison with the present results. The cited data are for the Reynolds number of 1.24×10^5, and they correspond to the Mach number of 0.47. In contrast to the present results, the decrease of the recovery factor at small nozzle-to-plate distances is not observed. It implies that the cooling effect at the small nozzle-to-plate distances is the inherent characteristic for the jets with shocks in them. Associated with the cooling effect at the small nozzle-to-plate distances, Fox and Kurosaka[15] proposed a mechanism of cooling named "shock-induced total temperature separation." As shown in Fig. 8, the present results for the underexpanded impinging jets are consistent with their hypothesis of the shock-induced cooling mechanism.

As the nozzle-to-plate distance is increased further, the recovery factor increases over unity. Similar behaviors also have been observed for subsonic jets by other investigators.[14,17,18] For the moderately underexpanded jet, rise of the recovery factor over unity occurs at $Z_P/D_{\mathrm{NE}} \cong 6.0$, and for the highly underexpanded jet, it occurs at $Z_P/D_{\mathrm{NE}} \cong 10.0$. This can be explained as follows: the static temperature of the jet is lower than the ambient temperature initially by the dynamic temperature. As the jet flows downstream, more amount of ambient air is entrained by mixing, and the static temperature of the jet increases with increasing nozzle-to-plate distance. As a result, the total temperature of the jet is increased comparing to the initial state.

The radial profile of recovery factor is also significantly dependent on the nozzle-to-plate distance. Figure 9 shows the radial profiles of recovery factor for various nozzle-to-plate distances at $P_e/P_a = 1.5$, which is the lowest underexpansion ratio tested in the present study. In the near field, the recovery factor has a maximum close to unity at the stagnation point and a minimum at $R/D_{\mathrm{NE}} \cong \pm 2.0$. As the

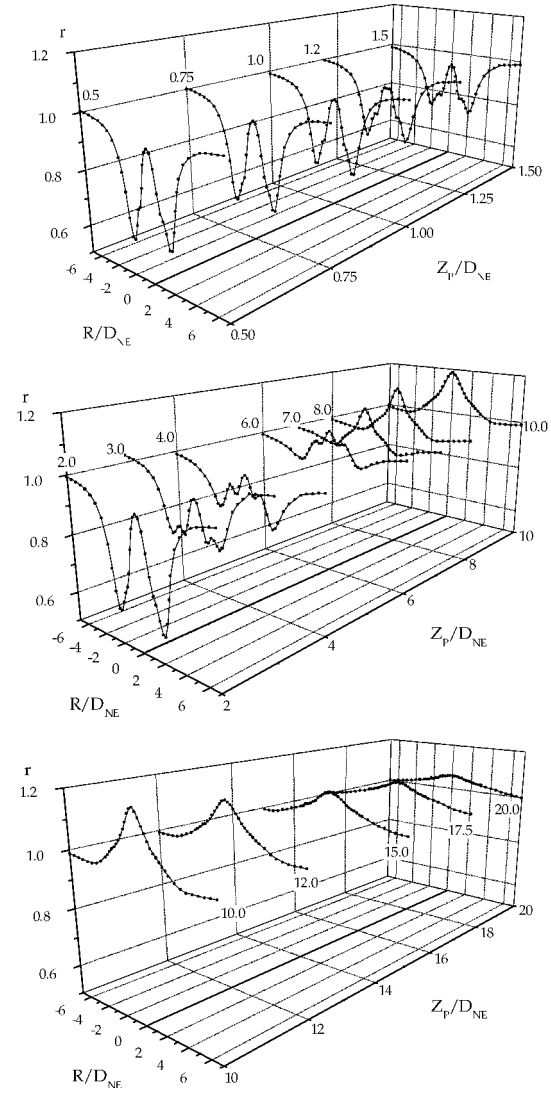

Fig. 9 Radial distributions of the recovery factor for various nozzle-to-plate distances at $P_e/P_a = 1.5$.

nozzle-to-plate distance increases, the maximum at the stagnation point increases over unity, while the minimum decreases in magnitude. As the local minimum appears outside of the shock layer, it seems not to be connected with the shock structure, and the similar results were also observed for subsonic jets.[17] The occurrence of the annular region of low recovery factor can be explained by the concept of vortex-induced total temperature separation, as discussed by Fox et al.[14] Secondary vortex rings are induced on the impingement plate by the approach of the primary vortex rings, which are formed around the nozzle lip and convected downstream. The region of low recovery factor is attributable to the total temperature separation induced by the secondary vortex rings. The existence of secondary vortex rings is dependent on the nozzle-to-plate distance: at a large nozzle-to-plate distance the primary vortex rings exist alone, and the secondary vortex rings disappear. This results in disappearance of the annular region of low recovery factor at a large nozzle-to-plate distance.

Figure 10 presents variation of the recovery factor profiles with underexpansion ratios at two nozzle-to-plate distances. A half-diameter ($Z_P/D_{NE} = 0.5$) is the smallest one within the present experimental conditions, and 20 diameters ($Z_P/D_{NE} = 20.0$) is the largest one. It is seen that the annular region of low recovery factor grows with increasing underexpansion ratio. The position of minimum moves increasingly outward, and the minimum value increases in magnitude as the underexpansion ratio increases. The minimum recovery factor at $Z_P/D_{NE} = 0.5$ is over 0.6 for $P_e/P_a = 1.5$, whereas it drops to about 0.4 for $P_e/P_a = 3.5$. At the large nozzle-to-plate distance of $Z_P/D_{NE} = 20.0$, the annular region of low recovery factor disappears, except for the highest underexpansion ratio of $P_e/P_a = 3.5$.

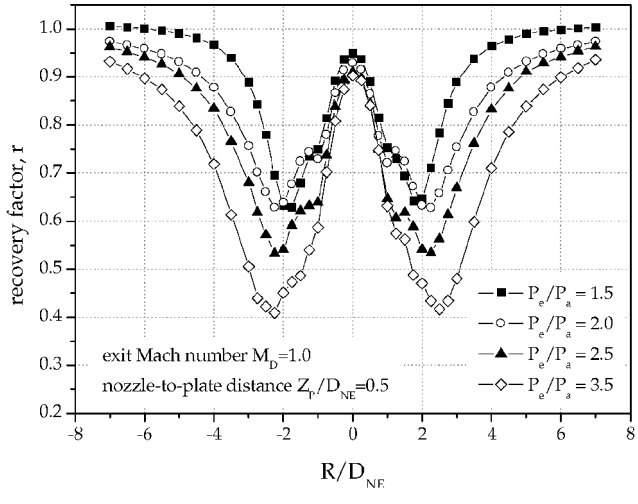

a) $Z_P/D_{NE} = 0.5$

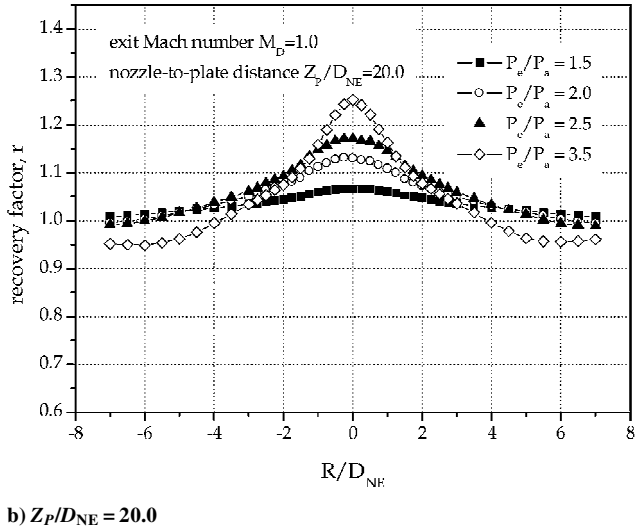

b) $Z_P/D_{NE} = 20.0$

Fig. 10 Comparison of the recovery factor for various underexpansion ratios.

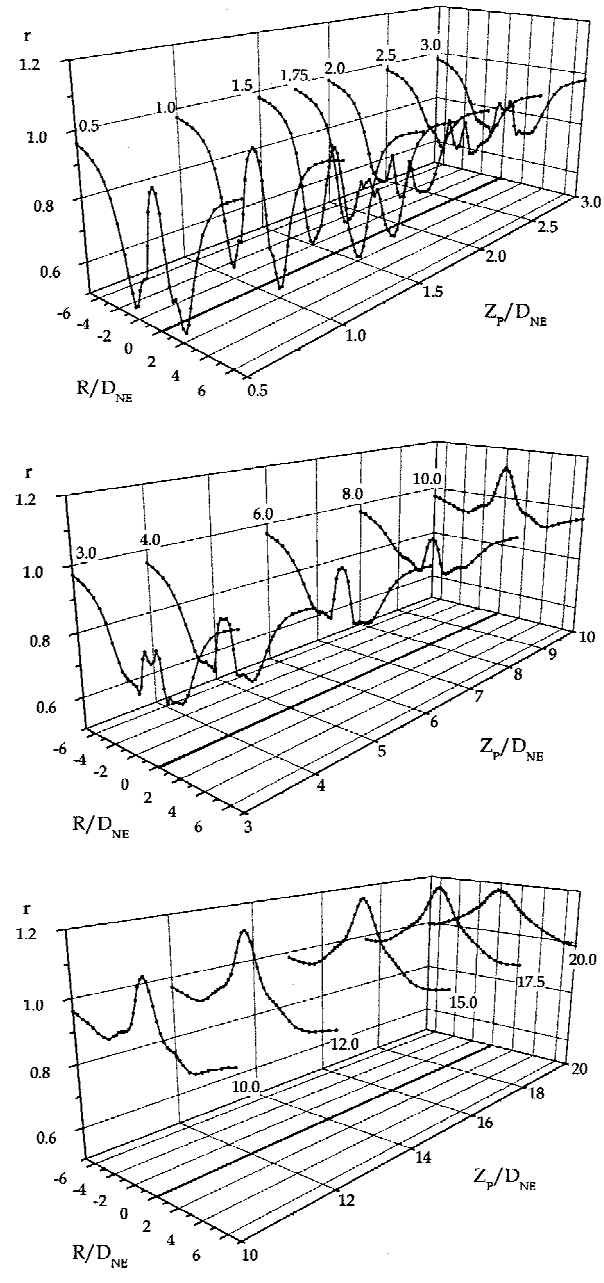

Fig. 11 Radial distributions of the recovery factor for various nozzle-to-plate distances at $P_e/P_a = 2.5$.

For $P_e/P_a = 2.0$ the radial distributions of recovery factor (not presented here) have similar variations with those for $P_e/P_a = 1.5$. For the highly underexpanded cases, however, the trends at small nozzle-to-plate distances are somewhat different from the moderately underexpanded cases, as shown in Fig. 11. For $P_e/P_a = 2.5$ the valleys commence to appear near the stagnation points at $Z_P/D_{NE} = 1.75$. They merge into a valley at $Z_P/D_{NE} = 2.0$, which results in formation of the region of low recovery factor in the stagnation region. It seems to be the effect of shock-induced cooling already mentioned. This effect of central cooling becomes stronger and persists farther downstream for the highest underexpansion ratio of $P_e/P_a = 3.5$.

VI. Conclusions

An experimental investigation has been conducted to examine heat-transfer characteristics of an axisymmetric underexpanded

sonic jet impinging on a flat plate. Distributions of the recovery factor and the surface pressure on the flat plate have been obtained in detail.

The results indicate that the interaction of shock waves in the free-jet with a stand-off shock ahead of the impingement plate depends strongly on the distance of the plate from the nozzle exit. Consequently, the surface pressure and recovery factor distributions on the impinging plate are changed significantly with the nozzle-to-plate distance.

Significant reduction of recovery factor, that is, cooling effect, occurs in the annular region near $R/D_{\mathrm{NE}} \cong 2.0$ when the plate is located at relatively short nozzle-to-plate distances and also in the stagnation region near $R/D_{\mathrm{NE}} \cong 0$ for the highly underexpanded cases. The cooling effect becomes stronger as the underexpansion ratio is increased. With increasing nozzle-to-plate distance, recovery factor increases gradually over unity. It means that heating effect occurs because the static temperature of jet increases by entrainment of warmer ambient air. It has been found that the recovery factor at the stagnation point varies from 0.35 up to over 1.25 for the highest underexpansion ratio of $P_e/P_a = 3.5$ within the present experimental range.

Acknowledgments

This research was supported by Ministry of Science and Technology through their National Research Laboratory program and by Agency for Defense Development.

References

[1]Ginzburg, I. P., Semiletenko, B. G., Terpigorev, V. S., and Uskov, V. N., "Some Singularities of Supersonic Underexpanded Jet Interaction with a Plane Obstacle," *Journal of Engineering Physics*, Vol. 19, 1973, pp. 1081–1084.

[2]Gubanova, O. I., Lucev, V. V., and Plastina, L. N., "Central Breakaway Zone with Interaction Between a Supersonic Underexpanded Jet and a Barrier," *Fluid Dynamics*, Vol. 6, 1973, pp. 298–301.

[3]Gummer, J. H., and Hunt, B. L., "The Impingement of a Uniform, Axisymmetric, Supersonic Jet on a Perpendicular Flat Plate," *The Aeronautical Quarterly*, Vol. 22, 1971, pp. 403–420.

[4]Kalghatgi, G. T., and Hunt, B. L., "The Occurrence of Stagnation Bubbles in Supersonic Impingement Flows," *The Aeronautical Quarterly*, Vol. 27, No. 3, 1976, pp. 169–185.

[5]Lamont, P. J., and Hunt, B. L., "The Impingement of Underexpanded, Axisymmetric Jets on Perpendicular and Inclined Flat Plates," *Journal of Fluid Mechanics*, Vol. 100, Pt. 3, Oct. 1980, pp. 471–511.

[6]Iwamoto, J., "Impingement of Under-Expanded Jets on a Flat Plate," *Journal of Fluids Engineering*, Vol. 112, No. 2, 1990, pp. 179–184.

[7]Carling, J. C., and Hunt, B. L., "The Near Wall Jet of a Normally Impinging, Uniform, Axisymmetric, Supersonic Jet," *Journal of Fluid Mechanics*, Vol. 66, Pt. 1, 1974, pp. 159–176.

[8]Pamadi, B. N., "On the Impingement of Supersonic Jet on a Normal Flat Surface," *The Aeronautical Quarterly*, 1982, pp. 199–218.

[9]Donaldson, C. D., and Snedeker, R. S., "A Study of Free Jet Impingement. Part 1. Mean Properties of Free and Impinging Jets," *Journal of Fluid Mechanics*, Vol. 45, Pt. 2, 1971, pp. 281–319.

[10]Iwamoto, J., and Deckker, B. E. L., "Development of a Flow when a Symmetrical Underexpanded Sonic Jet Impinges on a Flat Plate," *Journal of Fluid Mechanics*, Vol. 113, Dec. 1981, pp. 299–313.

[11]Kim, K. H., and Chang, K. S., "Three-Dimensional Structure of a Supersonic Jet Impinging on an Inclined Plate," *Journal of Spacecraft and Rockets*, Vol. 31, No. 5, 1994, pp. 778–782.

[12]Sakakibara, Y., and Iwamoto, J., "Numerical Study of Oscillation Mechanism in Underexpanded Jet Impinging on Plate," *Journal of Fluids Engineering*, Vol. 120, No. 3, 1998, pp. 477–481.

[13]Kim, B. G., Yu, M. S., Cho, Y. I., and Cho, H. H., "Distributions of Recovery Temperature on Flat Plate by Under-Expanded Supersonic Impinging Jet," *Journal of Thermophysics and Heat Transfer*, Vol. 16, No. 3, 2002, pp. 425–431.

[14]Fox, M. D., Kurosaka, M., Hedges, L., and Hirano, K., "The Influence of Vortical Structures on the Thermal Fields of Jets," *Journal of Fluid Mechanics*, Vol. 255, Oct. 1993, pp. 447–472.

[15]Fox, M. D., and Kurosaka, M., "Supersonic Cooling by Shock-Vortex Interaction," *Journal of Fluid Mechanics*, Vol. 308, Feb. 1996, pp. 363–379.

[16]Kline, S. J., and McClintock, F. A., "Describing Uncertainties in Single Sample Experiments," *Mechanical Engineering*, Vol. 75, No. 1, 1953, pp. 3–8.

[17]Goldstein, R. J., Behbahani, A. L., and Heppelmann, K. K., "Streamwise Distribution of the Recovery Factor and the Local Heat Transfer Coefficient to an Impinging Circular Air Jet," *International Journal of Heat and Mass Transfer*, Vol. 29, No. 8, 1986, pp. 1227–1235.

[18]Gardon, R., and Cobonpue, J., "Heat Transfer Between a Flat Plate and Jets of Air Impinging on It," *International Developments in Heat Transfer*, American Society of Mechanical Engineers, New York, 1962, pp. 454–460.